

Research Paper

Parkin deficiency exacerbate ethanol-induced dopaminergic neurodegeneration by P38 pathway dependent inhibition of autophagy and mitochondrial function



Chul Ju Hwang^a, Young Eun Kim^a, Dong Ju Son^a, Mi Hee Park^a, Dong-Young Choi^b, Pil-Hoon Park^b, Mats Hellström^{c,d}, Sang-Bae Han^a, Ki-Wan Oh^a, Eun Kyung Park^{e,*}, Jin Tae Hong^{a,*}

^a College of Pharmacy and Medical Research Center, Chungbuk National University, 194-31, Osongsangmyeong1-ro, Heungdeok-gu, Cheongju, Chungbuk 361-951, Republic of Korea

^b College of Pharmacy, Yeungnam University, 280, Daehak-ro, Gyeongsan, Gyeongbuk 712-749, Republic of Korea

^c Laboratory for Transplantation and Regenerative Medicine, Sahlgrenska Academy, University of Gothenburg, Gothenburg, Sweden

^d Department of Obstetrics and Gynecology, Sahlgrenska Academy, University of Gothenburg, Gothenburg, Sweden

^e Department of Obstetrics and Gynecology, College of Medicine, Daejeon St. Mary's Hospital, The Catholic University of Korea, 64 Daeheung-ro, Jung-gu, Daejeon 34943, Rep. of Korea

ARTICLE INFO

Keywords:

Autophagy
Mitochondrial function
Neurodegeneration
Park2
Parkinson disease (PD)

ABSTRACT

Parkinson's disease (PD) is a neurodegenerative disease characterized by selective degeneration of dopaminergic neurons in the substantia nigra. Parkin (which encoded by Park2), an E3 ubiquitin ligase, is the most frequently mutated gene that has casually been linked to autosomal recessive early onset familial PD. We tested the effect of Park2 on ethanol-induced dopaminergic neurodegeneration in Park2 knockout (KO) transgenic mice after chronic ethanol feeding. Male Park2 wild type (WT) and KO mice (8 weeks old) were fed on a Lieber-DeCarli diet containing 6.6% ethanol for 2 weeks, and compared their responses. We found that knockout of Park2 exacerbates ethanol-induced behavioral impairment as well as dopamine depletion. In the mechanism study, we found that knockout of Park2 increased reactive oxygen species (ROS) production, mitophagy formation, mitochondrial dysfunction, and expression of pro-apoptotic proteins, but decreased expression of pro-autophagic proteins. Knockout of Park2 also increased ethanol-induced activation of p38 mitogen-activated protein kinase. In addition, ROS production, mitophagy formation, mitochondrial dysfunction, and expression of pro-apoptotic proteins were increased, but expression of pro-autophagic proteins were decreased by a treatment of ethanol (100 μ M) in Park2 siRNA-transfected PC12 cells (5 μ M). Moreover, the exacerbating effects of Park2 deletion on ethanol-induced ROS generation, mitophagy, mitochondrial dysfunction as well as cell death were reduced by p38 specific inhibitor (SB203580) in vitro (10 μ M) and in vivo 10 mg/kg). Park2 deficiency exacerbates ethanol-induced dopaminergic neuron damage through p38 kinase dependent inhibition of autophagy and mitochondrial function.

1. Introduction

Park2, which encodes Parkin, is the most frequently mutated gene that has casually been linked to autosomal recessive early onset familial Parkinson's disease (PD) [1]. Abnormalities of Parkin have also been described in sporadic PD [2]. Parkin is an E3 ubiquitin ligase that provides specificity for the process of tagging proteins with ubiquitin for degradation in the ubiquitin proteasome system [3]. Evidence implicating a direct role for the ubiquitination in PD came from the association of genetic mutations in the parkin gene with familial parkinsonism [1], and several studies demonstrated that parkin acts as a ubiquitin ligase

associated with proteasomal degradation [4–6]. This property of parkin thus directly related with ubiquitination for dopaminergic neuronal survival [7]. The exact mechanism by which Parkin causes PD-like syndromes and why dopaminergic neurons are primarily affected by a ubiquitously expressed mutation remain unclear [8,9]. However, several studies suggest that Parkin interacts with PINK1 (PTEN-induced putative kinase 1; also known as PARK6), another gene mutated in autosomal recessive familial form of PD [10] to regulate mitochondrial biology, and alters mitochondrial dynamics [11].

Recently, a study performed with cultured cells has shown that Parkin can mediate autophagy on damaged mitochondria [12]. The

* Corresponding authors.

E-mail address: jinthong@chungbuk.ac.kr (J.T. Hong).

<http://dx.doi.org/10.1016/j.redox.2016.12.008>

Received 4 October 2016; Received in revised form 9 November 2016; Accepted 2 December 2016

Available online 08 December 2016

2213-2317/ © 2016 The Authors. Published by Elsevier B.V.

This is an open access article under the CC BY-NC-ND license (<http://creativecommons.org/licenses/by-nc-nd/4.0/>).

relation between Parkin and mitochondrial biology was first established in *Drosophila*, which displayed impairment in mitochondrial function and neuronal loss in an age-dependent manner when rendered deficient for Parkin [13]. Likewise, similar mitochondrial defects were exhibited in Park2 knockout (KO) mouse models although only mice with conditional KO of Park2 recapitulate parkinsonian phenotype and striatonigral degeneration [14]. More recently, post-mortem brain tissues of PD patients also confirmed the involvement of altered mitochondrial pathologies in the disease process [15]. Parkin has a protective effect against a diversity of insults. More importantly, viral over-expression of parkin protected midbrain dopaminergic neurons against acute α -synuclein damage in primary culture [16] and rat brain [17] as well as in *Drosophila melanogaster* [18]. It was also found that parkin expression was protective against 6-hydroxydopamine neurotoxicity in rat brain [19]. Parkin over-expression also protected SH-SY5Y human neuroblastoma cells against oxidative dopamine neurotoxicity [20]. The neuroprotective function of parkin has also been suggested to result from its selective recruitment to damaged mitochondria, where it promotes the autophagic removal of the reactive oxygen species (ROS)-generating organelles [12].

ROS are chemically reactive chemical species containing oxygen such as peroxides, superoxide, hydroxyl radical, and singlet oxygen [21]. In a biological context, ROS have important roles in cell signaling and homeostasis [22]. However, during times of environmental stress, ROS levels can increase, and this may result in significant damage to cell structures [22]. It has been reported that hydrogen peroxide (H_2O_2) is able to activate the p38 kinase to induce apoptosis [23]. In PD conditions, oxidative stress is a major cause of neuronal death. Studies with PD-like symptoms elicited animal models have shown that extracellular superoxide $\cdot O_2^-$ production results in the activation of microglial cells which subsequently attack neighboring dopaminergic neurons [24]. Many studies have already demonstrated that several kinds of ROS can induce the activation of the mitogen-activated protein kinase (MAPK) pathways [25]. A number of evidence suggests that induction of ROS production can activate MAPK pathways in multiple cell types [25,26]. The p38 MAPK activation was also higher in PD models and it was implicated in the mechanism of neuronal cell death [27]. Indeed, p38 phosphorylation induces the expression of the pro-apoptotic protein Bax [28], in dopaminergic neurons of the mice midbrain [29]. In addition, p38 MAPK is a critical link between Fas and the mitochondrial death pathway. A recent study has suggested that the activation of p38 MAPK can induce mitochondrial death pathway through Fas-induced apoptosis [30]. Moreover, p38 is believed to regulate not only apoptosis but also autophagy. p38 MAPK is an essential effector for modulating apoptosis or autophagy under ER stress. Recently study indicated that chemical or protein induced-p38 activation suppressed autophagy but promoted apoptosis [31,32]. Together, these suggest that MAPK signaling pathways contribute to neuronal death through functional deficiencies of mitochondria in the pathogenesis of PD.

Ethanol (EtOH) is the most psychoactive substance used after caffeine. Chronic alcoholism is a major public health problem and causes multi-organ diseases and toxicity. Although the liver metabolizes the majority of EtOH ingested, it has intoxicating effects in brain diseases [33]. Chronic alcohol intake is associated with several degenerative and inflammatory processes in the central nervous system (CNS) [34]. EtOH promotes oxidative stress by increasing ROS, mostly superoxide ($\cdot O_2^-$) formation as well as decreasing cellular defense mechanisms. A recent study suggests that EtOH-induced defects in the mitochondrial function may promote in apoptotic cell death disease models [35]. The CNS is vulnerable to free radical damage because the brain has a high oxygen consumption, abundant lipid content, and the relative paucity of antioxidant enzymes as compared with other tissues [36]. Therefore, in the present study, we demonstrate that Parkin deficiency exacerbate EtOH-induced oxidative damage on brain through p38 signaling-dependent dysfunction of mitochondria. In this

study, Park2 KO mice have a lower number of nigral dopaminergic neurons than WT mice. Moreover, EtOH-induced impairments were more severe on the nigrostriatal dopaminergic system through p38 signal dependent dysfunction of mitochondria and mitophagy.

2. Materials and methods

2.1. Animal

The age 4–5 month-old, sex (male) and weight (26–27 g) matched wild type (C57BL/6) mice and Park2 KO mice were maintained in accordance with the guidance of the National Institute of Toxicological Research for the care and use of laboratory animals. All of the experimental procedures were approved by the Animal Care and Use Committee (IACUC) of Chungbuk National University (approval number: CBNUA-929-16-01). The C57BL/6 and Park2 KO mice were purchased from The Jackson Laboratory (Bar Harbor, Maine 04609). All mice were housed in a room that was automatically maintained at 21–25 °C and at relative humidity (45–65%) with a controlled light–dark cycle. Park2 KO mice and WT mice were randomly divided into four groups ($n=8$ per group). Each group of mice received 2 different types of liquid diets for 10 days: (1) paired-fed standard diet with water (pair-fed); (2) Alcohol diet with ethanol (EtOH-fed). EtOH comprised 35.8% of total calories in mice receiving EtOH. Liquid diets (pair-fed and EtOH-fed) were based upon the Lieber-DeCarli EtOH formulation and were purchased from DYETS Inc. (Bethlehem, PA). The EtOH concentration of 6.6% was kept thereafter for 8 days. After 8 days of feeding, the mice were sacrificed.

2.2. Behavioral tests

We performed behavioral tests to examine whether there was a difference in the EtOH-caused behavioral deficit between C57BL/6 and Park2 KO mice. Rotarod, pole and gait tests were conducted as the behavioral tests.

2.3. Rotarod test

Motor performance and coordination were examined using the Rotarod treadmill (MED Associates Inc., St. Albans, VT.), consisting of a 3.6-cm diameter cylindrical treadmill connected to a computer-controlled stepper motor as described previously [37]. When the animal falls off the rotating drum, individual sensors sense it, and automatically record the length of time spent on the treadmill (in seconds). Mice were trained two consecutive days before in acceleration mode (2–20 rpm) over 5 min. The training was repeated with a fixed speed (10 rpm) until the mice were able to stay on the rod for at least 300 s. If animals did not pass the trainings, they were excluded from further experiments.

2.4. Pole test

The rough-surfaced wooden pole (1 cm in diameter, 55 cm in height) was vertically placed on the floor of home cage. Upon being placed head-upward on top of the pole, mice turned downward and descended back to their home cages. Prior to the test trials, mice were acclimatized to the pole over three trials with intervals of 30 s between the trials. On the test trials, total time for them to orient downward and descend to the floor was assessed. The test trials were performed three times per animal and average values from three examinations were used for each animal.

2.5. Gait test

The forelimbs and hindlimbs were painted with ink and animals were placed on a bright runway (4.5 cm wide, 42 cm long, with walls

12 cm high) and were allowed to run toward a dark goal box (20×17×10 cm). Mice were subject to two training trials to be acclimatized at the environment. A single test trial was performed and stride length was measured as the distance between successive paw prints. Data was presented as the average of five strides for each animal.

2.6. Collection and preservation of brain tissues

After the behavior tests, mice were sacrificed with CO₂ gas and then perfused with phosphate-buffered saline (PBS). The brains were immediately removed from the skull, and the tissues were stored at –80 °C until biochemical analysis.

2.7. HPLC analysis of dopamine and its metabolite

Dopamine and metabolites in the striatum were measured by HPLC. Briefly, tissues were sonicated in chilled 0.1 M perchloric acid containing dihydroxybenzylamine as an internal standard. After centrifugation (15,000×g, 30 min, 4 °C), the supernatant was diluted with mobile phase (75 mM of NaH₂PO₄, 1.7 mM Octane sulfonic acid, 10% methanol, pH 3.0), and 10 µl of sample was isocratically eluted through a 80×4.6 mm C18 column (Waters Associates, Milford, MA) with a flow rate of 1.5 ml/min. Neurochemicals including dopamine, 3,4-dihydroxyphenylacetic acid (DOPAC) were detected by a two-channel electrochemical detector (Waters Associates) at a potential of 1.5 mV. Concentrations were normalized by wet tissue weight.

2.8. Immunohistochemistry and immunofluorescence

Tissue Section, 5 mm thick, were used for immunohistochemistry (and immunofluorescence) examinations. Paraffin-embedded sections were deparaffinized and rehydrated, washed in distilled water, and then subjected to heat-mediated antigen retrieval treatment. Endogenous peroxidase activity was quenched via incubation in 1% hydrogen peroxide in methanol for 30 min, followed by clearing with PBS for 5 min. The sections were blocked for 30 min with 3% normal horse/goat serum diluted in PBS. These sections were incubated overnight with the appropriate antibodies. After washing in PBS, the sections were incubated in biotinylated goat anti-mouse/rabbit IgG antibody (1:1000 dilution; Vector Laboratories, Burlingame, CA, USA) for 1 h at room temperature. The sections were subsequently washed and incubated with avidin-conjugated peroxidase complex (ABC kit, 1:200 dilution; Vector Laboratories) for 30 min, followed by PBS washing. The peroxidase reaction was performed in PBS using 3, 3'-diaminobenzidine tetrahydrochloride (DAB, 0.02%) as the chromogen. Finally, sections were dehydrated in ethanol, cleared in xylene, mounted with Permount (Fisher Scientific, Waltham, MA, USA), and evaluated via light microscopy (Olympus, Tokyo, Japan). For immunofluorescence examination, sections were incubated with anti-rabbit secondary antibody labeled with Alexa-Fluor 488 (1:400 dilution; Invitrogen, Carlsbad, CA, USA) or anti-mouse secondary antibody labeled with Alexa-Fluor 568 (1:400 dilution; Invitrogen) for 2 h at room temperature. The final images were acquired using a confocal laser scanning microscope (TCS SP2, Leica Microsystems AG, Wetzlar, Germany).

2.9. Analysis of the number of TH-positive neurons and density of TH-positive fibers

The total number of TH-positive cells was counted in sections using the optical fractionator method for unbiased cell counting as described previously with slight modifications [38]. Briefly, every sixth section throughout the entire extent of the substantia nigra was picked, and immunostaining for TH was performed. The number of TH-positive neurons was counted by using a computer-assisted image analysis

system consisting of a Zeiss Axioskop2 Plus photomicroscope equipped with an MS-2000 (Applied Scientific Instrumentation, Eugene, OR) computer-controlled motorized stage, a Sony DXC-390 video camera, a DELL GX260 workstation, and the Optical Fractionator Project module of the BIOQUANT Stereology Toolkit Plug-in for BIOQUANT Nova Prime software (BIOQUANT Image Analysis Corporation, Nashville, TN). The substantia nigral region was observed at a low magnification (10× objective) and was outlined by using a set of anatomical landmarks. The cell number was counted at a high magnification (40× objective). The total number of neurons was automatically calculated by the software. For determining striatal TH-positive fiber density, we picked six striatum-containing sections covering the entire head and tail of the striatum from each animal. To prevent non-specific staining, a blocking step was included. Sections were incubated for 2 h at room temperature with 5% BSA (in PBS). Sections were then incubated overnight at 4 °C with the primary antibody in blocking solution (5% BSA). TH-positive fiber density was measured by using Bioquant Image Analysis software. All images are converted to a gray scale for standardizing white balance. Each value was corrected for non-specific background by subtracting the optical density of the corpus callosum.

2.10. Western blot analysis

The brain tissues were homogenized with lysis buffer (PRO-PREP; iNtRON, Sungnam, Korea; n=8 mice per group) and centrifuged at 2500×g for 15 min at 4 °C. Equal amounts of total protein (20 µg) isolated from brain tissues were resolved on 8% or 10% sodium dodecyl sulfate polyacrylamide gels and then transferred to nitrocellulose membranes (Hybond ECL; Amersham Pharmacia Biotech, Piscataway, NJ). Membranes were incubated at 4 °C for 12 h with the following specific antibodies: anti-GFAP, anti-iba1 (1:1000; Abcam, Inc., Cambridge, MA), anti-COX-2, anti-p38, anti-p-p38, anti-p-JNK, anti-JNK, anti-p-ERK, anti-ERK (Cell Signaling Technology, Inc., Beverly, MA), anti-MAO B (1:1000; Santa Cruz Biotechnologies, Inc., Santa Cruz, CA), and anti-β-actin (1:2500; Santa Cruz Biotechnologies, Inc., Santa Cruz, CA). Blots were then incubated at room temperature for 2 h with corresponding peroxidase-conjugated anti-goat/mouse/rabbit (1/2000; Santa Cruz Biotechnology, Inc., Santa Cruz, CA). Immunoreactive proteins were detected using an enhanced chemiluminescence [39] Western blotting detection system. The relative density of the protein bands was scanned densitometrically using My Image (SLB, Seoul, Korea) and quantified by Lab Works 4.0 (UVP, Upland, CA).

2.11. TUNEL assay

DNA fragmentation was examined with terminal deoxynucleotidyl transferase-mediated FITC–dUDP nick-end labeling (TUNEL). TUNEL assays were performed using the *in situ* Cell Death Detection Kit (Roche Diagnostics GmbH, Mannheim, Germany) according to the manufacturer's instructions. In brief, after fixation of 25-mm cryosections with 4% paraformaldehyde, and treatment with 0.1% NaBH₄ and 0.1 Triton X-100, the slides were incubated for at least 1 h with a reaction mixture containing deoxynucleotidyl transferase and FITC–dUDP (Roche, Reinach, Switzerland). For 40, 60-diamidino-2-phenylindole dihydrochloride (DAPI) staining, the slides were incubated for 15 min at room temperature in the dark with a mounting medium for fluorescence containing DAPI (Vector Laboratories, Cambridgeshire, UK). The tissues were then examined through a fluorescence microscope (Leica Microsystems AG, Wetzlar, Germany), and the nuclei were visualized via DAPI staining.

2.12. Mitochondrial membrane potential

Mitochondrial membrane potential was assessed using JC-1, a cationic dye that exhibits potential-dependent accumulation and for-

mation of red fluorescent J-aggregates in mitochondria. In contrast, changes in plasma membrane potential do not affect the JC-1 status. The JC-1 monomer accumulates in the cytoplasm where it produces a green fluorescence. Formation of J-aggregates in the mitochondria is indicated by a fluorescence emission shift from green (525 nm) to red (590 nm). The JC-1 monomer (green) and the J-aggregate (red) were detected separately in FL1 (emission, 525 nm) and FL2 (emission, 590 nm) channels, respectively.

2.13. Measurement of oxidative stress

Hydrogen peroxides were measured according to the manufacturer's instructions (Cell Biolabs, San Diego, CA). Total glutathione (GSH), and Malondialdehyde (MDA) were measured according to the manufacturer's instructions (Cayman chemical, Ann Arbor, MI). To perform assay, the brain tissues and PC-12 cells were homogenized, then normalized to protein concentration. Superoxide production in brain tissue and PC-12 cells were detected by dihydroethidium (DHE) staining (Sigma-Aldrich). Brain sections and PC-12 cells were incubated with 10 μ M DHE for 45 min at 37 °C in a humidified chamber protected from light. The average fluorescence intensity of the nuclei was then analyzed using Image Pro-Plus software (Media Cybernetics, Inc., Rockville, MD). Protein carbonyl content was measured as a marker of oxidative damage to proteins [40,41]. The contents of protein carbonyl were measured using a Protein Carbonyl Content Assay Kit (Abcam, Inc., Cambridge, MA) following the manufacturer's protocol. They were determined the hydrazone derivatives between

360 nm. Data are expressed as nmol carbonyls/mg protein.

2.14. Statistical analysis

All statistical analysis was performed with GraphPad Prism 4 software (Version 4.03; GraphPad software, Inc., San Diego, CA). Group differences in the Rotarod test, pole test and gait test were analyzed using two-way ANOVA followed by Dunnett's *post hoc* test. All values are presented as mean \pm SEM. Significance was set at $p < 0.05$ for all tests.

3. Results

3.1. Effect of Park2 knockout on behavioral impairments

We examined the effect of Park2 deletion on behavior disorder. Park2 KO mice did not show any overt behavioral impairment in comparison to C57BL/6 Park2 WT mice between the pair-fed groups. The rotarod test was carried out to assess their coordination capability. EtOH consumption significantly decreased latency on the rotarod in both Park2 WT and Park2 KO mice. However, the latency to fall in EtOH-fed Park2 KO mice (19.8 ± 7.13 s) was significantly decreased compared to EtOH-fed Park2 WT mice (40.3 ± 12.15 s); (F value=14.57) (Fig. 1A). Next, we conducted the pole test and measured the time it took to descend from the top of the pole to the floor. Elongation of the parameter is considered to reflect bradykinesia. Paired groups did not show any significant difference on behavior disorder in both Park2 WT and Park2 KO mice. In contrast, the time to descend

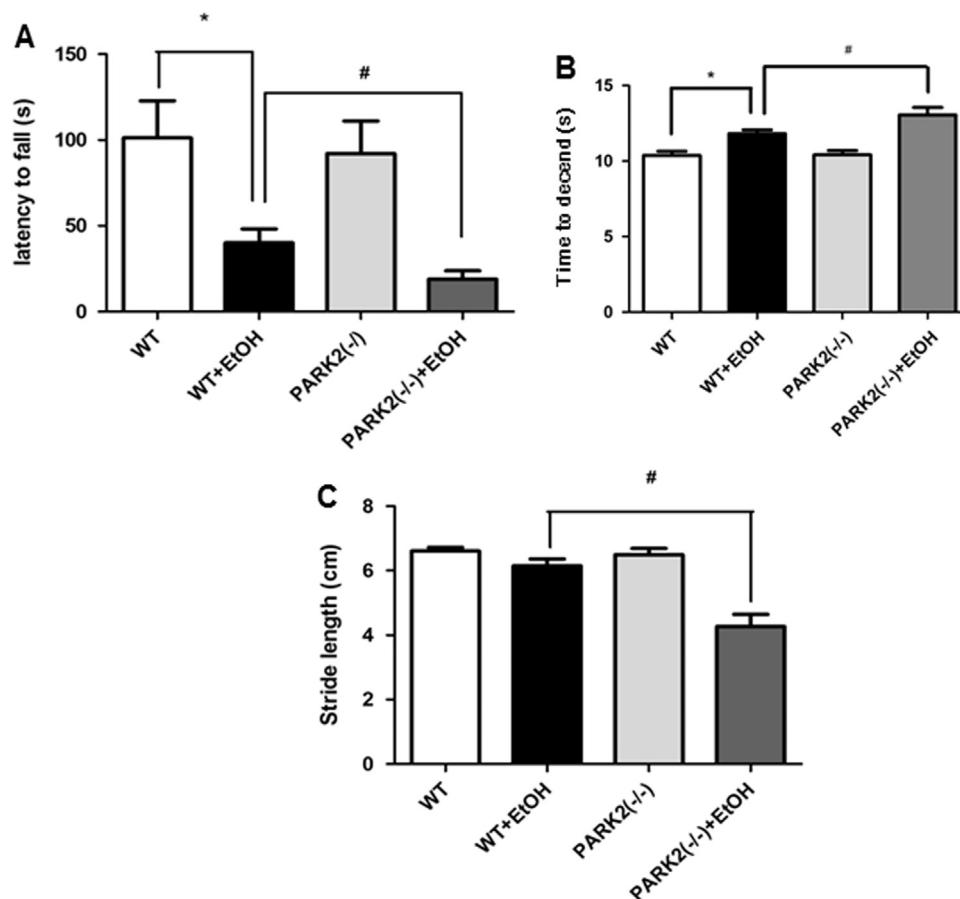


Fig. 1. Park2 deficiency exacerbates ethanol-induced behavior disorder. Performance on the rotarod is impaired by ethanol treatment in both Park2 WT and KO mice. However, the impairment is more obvious in Park2 KO mice (A). MPTP-induced bradykinesia (in the performance of the pole test when animals descended the length of the pole) is more observed in Park2 KO mice (B). Stride length of forelimb is more shortened by ethanol consumption in Park2 KO (C). Each value is presented as mean \pm SD from eight mice. *, $p < 0.05$; Significant difference from control mice and #, $p < 0.05$; Significant difference between the Park2 WT and KO mice.

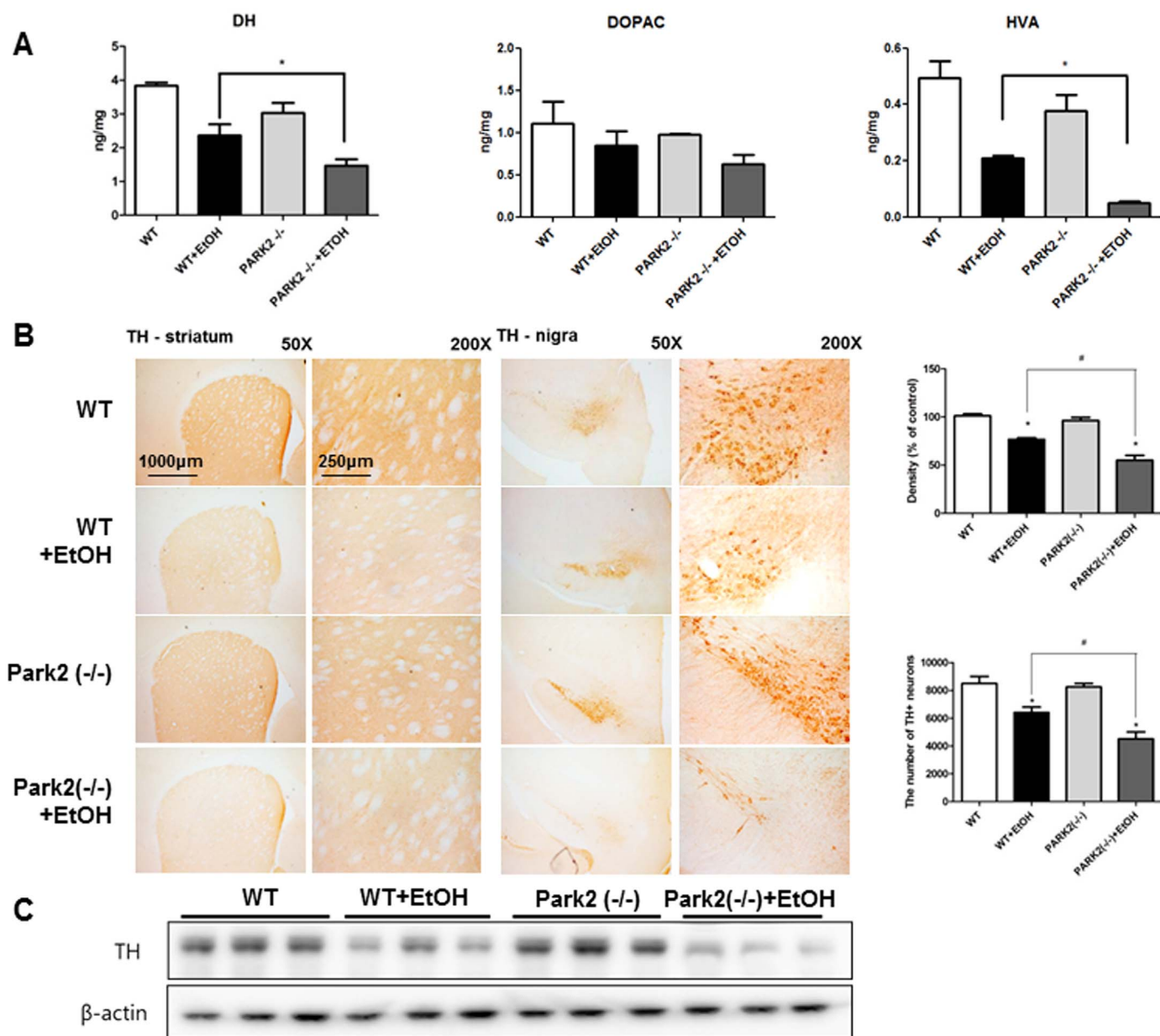


Fig. 2. Park2 deficiency amplifies EtOH-induced dopaminergic neurodegeneration. Levels of dopamine (A), DOPAC and HVA (metabolite of dopamine) (B) in the mice brain between four groups were determined by HPLC. The effect of Park2 KO on TH-positive neurons was measured by immunohistochemical analysis. The two sections represent mice brain (striatum and substantia nigra) incubated with anti-TH+ primary antibody and the biotinylated secondary antibody ($n=3$). The representative stained tissues were viewed with a microscope (X50 or 200). EtOH-induced loss of TH-positive fibers in the striatum is more prominent in Park2 KO mice (B). The graph represents density of tissue sections and the number of TH-positive neuronal cells. In addition, there is a significant decrease in the expression of TH in the whole brain of EtOH-fed Park2 KO mice (C). Total number of cells was calculated in each section. All values are the mean \pm S.D. from three mice brains. *, $p < 0.05$: Significant difference from control mice and #, $p < 0.05$: Significant difference between the Park2 WT and KO mice.

was significantly decreased in EtOH-fed Park2 KO mice (13.05 ± 0.51 s) compared to EtOH-fed Park2 WT mice (11.83 ± 0.24 s); (F value=4.58) (Fig. 1B). When the stride length test was performed, results showed that EtOH-fed had shortened fore limb stride length (Fig. 1C). The stride length of the hind limb was shortened more in EtOH-fed Park2 KO mice (4.2 ± 0.1 cm) compared to EtOH-fed Park2 WT mice (6.6 ± 0.3 cm); (F value=3.89). There was no significant difference in behavior disorders between Park2 KO and Park2 WT mice between the pair-fed mice of the two groups.

3.2. Effect of Park2 knockout on dopaminergic neurodegeneration

We evaluated EtOH-neurotoxicity on dopamine deletion using HPLC analysis. HPLC analysis for neurochemicals including dopamine

and its metabolite DOPAC and HVA was conducted with the striatum tissues. Absence of Park2 showed lower levels of dopamine and its metabolites in the striatum after EtOH feeding (Fig. 2A). Immunohistochemical stainings for TH showed there were abundant TH-positive fibers in the striatum and substantia nigra of Park2 KO and Park2 WT mice between the pair-fed groups. When the mice were fed the EtOH diet, the number of TH-positive neurons was significantly lowered in the substantia nigra of both Park2 WT and Park2 KO mice, as determined by immunostaining and stereological counting (Fig. 2B). Population of the dopaminergic neuron was lower in EtOH-fed Park2 KO mice compared to EtOH-fed Park2 WT mice. Consistent with this, density of TH-positive fibers in the striatum following EtOH consumption was lower in Park2 KO mice compared to Park2 WT mice (Fig. 2B).

3.3. Effect of Park2 knockout on the autophagy and mitochondrial function

LC3 is widely used to determine for autophagy. LC3 is known to exist in two forms: LC3-I, which is found in the cytoplasm and LC3-II, which is membrane-bound and is converted from LC3-I, to initiate formation and lengthening of the autophagosome [42]. One approach is to detect LC3 conversion (LC3-I to LC3-II) by immunoblot analysis because the LC3-II is clearly correlated with the number of autophagosomes. However, owing to several problems, summation of LC3-I and LC3-II for ratio determinations, may not be appropriate, and rather, the amount of LC3-II can be compared between samples [43]. In order to compare the amount of mitophagy without false positive results, we measured the ratio of LC3-II/TOM20. Double immunofluorescence staining showed that significantly higher number of immunoreactive cells against TOM20 and LC3 were observed in the brains of EtOH-fed Park2 KO mice than those of EtOH-fed Park2 WT mice. TOM20 and LC3 were normally expressed in normal-fed groups brain. TOM20 was highly expressed and a large number of cells were double positive for LC3 in the brains of EtOH-fed Park2 WT mice. However, expression of

TOM20 was decreased and a small number of cells were double positive for LC3 in EtOH-fed Park2 KO mice (Fig. 3A). In order to quantify the fluorescence, we measured the ratio of TOM20 and LC3/DAPI signals (Fig. 3B). In addition, effect of Park2 KO on mitochondrial membrane potential loss in the brain was examined by JC-1 staining. Changes in the mitochondrial membrane potential were determined by red versus green fluorescence using JC-1 dye where healthy mitochondria give out fluorescence because of J aggregates of JC-1 dyes, while damaged cells show green fluorescence because of the lack of mitochondrial membrane potential. The ratio between the measurements at wavelengths of 590 nm (red) and 540 nm (green) fluorescence showed a significantly higher number of damaged cells in the parkin siRNA-transfected (5 μ M) PC-12 cells against EtOH treatment (Fig. 3C). Similar to double staining data, expressions of TOM20 and LC3 were significantly lowered in EtOH-fed Park2 KO mice compared to EtOH-fed Park2 WT mice (Fig. 3D). In addition, the ratio of LC3-II/TOM20 was significantly lowered in EtOH-fed Park2 KO mice compared to EtOH-fed Park2 WT mice (Fig. 3E). The results suggest that the absence of Park2 leads to the down-regulation of autophagy through decreased mitochondrial function.

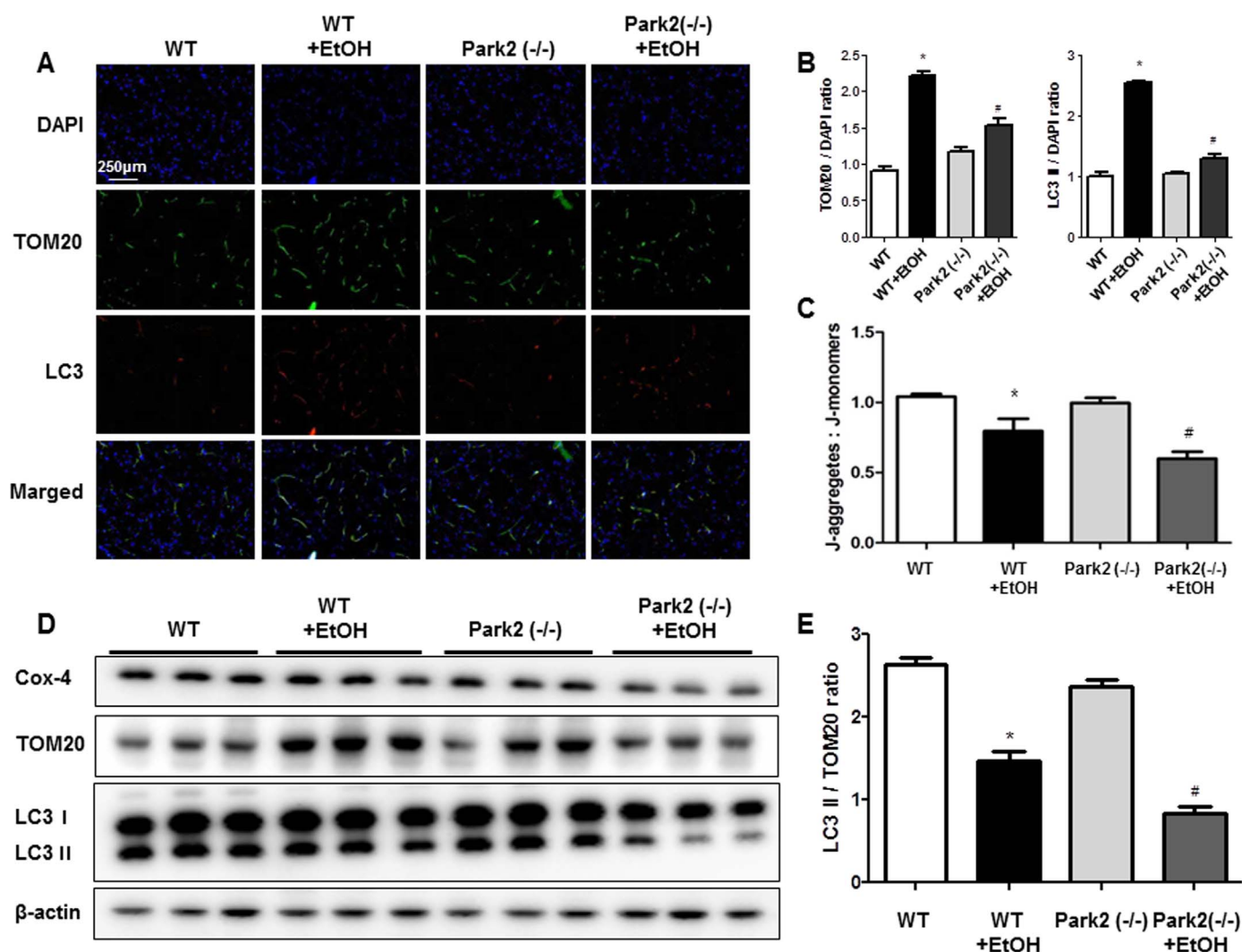


Fig. 3. Park2 deficiency amplifies the EtOH-induced dysfunction of mitochondrial autophagy. To evaluate relation of Park2 and mitochondrial autophagy, double immunofluorescence staining of TOM20 with LC3 was performed. Brain sections were incubated with specific antibodies against TOM20 (green) and LC3 (red) proteins. The representative stained tissues were viewed with a microscope (X100) (A). The ratio of TOM20 or LC3II/DAPI was measured for quantification of fluorescence (B). Mitochondrial membrane potential in brains after EtOH-induced injury. Results are expressed as the ratio of the aggregate-to-monomeric form of JC-1 (C). Expression of Cox-4, TOM20 and LC3 was also examined by specific antibodies in the brain (D). The ratio of LC3 II/TOM20 was measured for comparison of mitophagy (E). All values are the mean \pm S.D. from three mice brains. *, < 0.05: Significant difference from control mice and #, p < 0.05: Significant difference between the Park2 WT and KO mice.

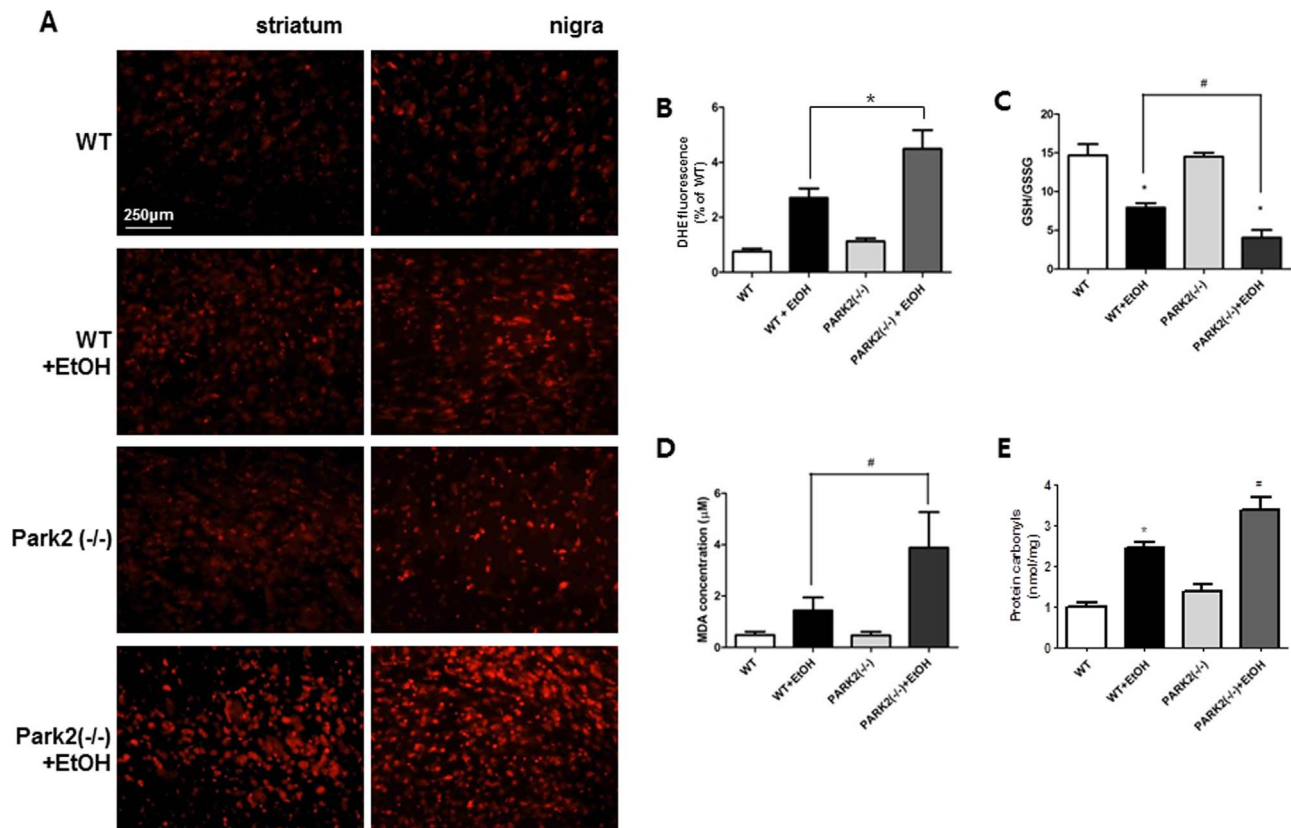


Fig. 4. Park2 deficiency amplifies the EtOH-induced oxidative stress. The intensity of DHE staining was significantly increased in the EtOH-fed Park2 KO mice, suggesting increased superoxide production. DHE staining of the four mice brains. The representative stained tissues were viewed with a microscope (X100) (A). Accumulation of superoxide were measured by DHE positive fluorescence (B). Effect of park2 KO on the GSH/GSSG content in brains of four groups. Oxidative stress was assessed by measuring the GSH/GSSG ratio (C). In order to determine whether mitochondrial damage and cytotoxicity were related to oxidative stress, we measured the levels of lipid oxidation products (MDA) (D) and protein carbonyl contents (E) in mice brain. All values are the mean \pm S.D. from three mice brains. *, $p < 0.05$: Significant difference from control mice and #, $p < 0.05$: Significant difference between the Park2 WT and KO mice.

3.4. Effect of Park2 knockout on the generation of ROS

In order to test superoxide production in brains, we performed dihydroethidium (DHE) staining. The reactive fluorescence of DHE in the brain was increased to about 321% in EtOH-fed Park2 WT mice group compared to non-treated park2 WT mice group, but it was greatly increased to about 463% in the EtOH-fed Park2 KO mice group (Fig. 4A and B). The total glutathione level was depleted to about 51% in EtOH-fed Park2 WT mice group, but was depleted to about 69% in EtOH-fed Park2 KO mice group (Fig. 4C). In addition, MDA concentration was much higher in EtOH-fed Park2 KO mice compared to EtOH-fed Park2 WT mice (Fig. 4D). Consistent with these data, protein carbonyl contents were much higher in EtOH-fed Park2 KO mice compared to EtOH-fed Park2 WT mice (Fig. 4E).

3.5. Effect of Park2 knockout on the apoptosis

To investigate apoptosis of neuronal cells in the brain, we performed TUNEL assay in the brain sections. In the brains of EtOH-fed groups, TUNEL-positive apoptotic cells were frequently observed and an indication of apoptosis was significantly higher in Park2 KO mice than that of Park2 WT mice. The number of apoptotic cells (DAPI-positive TUNEL-stained cells) in the brain was increased to about 38% in EtOH-fed Park2 WT mice group, but it increased to about 58% in the EtOH-fed Park2 KO mice group (Fig. 5A). The expression of cell death regulatory proteins including caspases-3, -8 and -9 as well as Bax and Bcl-2, the expression of apoptotic proteins was investigated by Western blots. The expression of pro-apoptotic proteins, Bax and cleaved form of caspase-3, -8, -9 were greatly increased in EtOH-fed

Park2 KO mice brain compared to that in EtOH-fed WT mice brain. However, the expression of Bcl2 was significantly decreased in EtOH-fed Park2 KO mice brain (Fig. 5B).

3.6. Effect of Park2 knock down on EtOH-induced autophagy, mitochondrial function and ROS generation in PC-12 cells

To further examine the regulating effect of Park2 on autophagy and ROS generation, the Park2 gene expression was knocked down by parkin siRNA-transfection (5 μ M) in PC-12 cells. First, we investigated protein expression of Park2 in parkin siRNA transfected PC-12 cells treated with EtOH. We observed that expression of Parkin was significantly lower in siRNA transfected PC-12 cells (Fig. 6A). The immunoblot data showed that expression of COX4, LC3 and TOM20 were significantly increased by EtOH treatment, but these expressions were decreased in parkin siRNA-transfected PC-12 cells (Fig. 6A). In addition, the ratio of LC3-II/TOM20 was significantly increased by EtOH treatment, but this ratio was decreased in parkin siRNA-transfected PC-12 cells (Fig. 6B). To evaluate autophagy, which can promote cell survival, we investigated protein expression of autophagy markers. Double immunofluorescence staining showed a significantly lower number of immunoreactive cells against TOM20 and LC3 were observed in the parkin siRNA-transfected PC-12 cells against EtOH treatment (Fig. 6C). In addition, the effect of Park2 knock-down on mitochondrial membrane potential loss in PC-12 cells was investigated by JC-1 staining followed by fluorescence microscopy. Changes in the mitochondrial membrane potential were determined by red versus green fluorescence using JC-1 dye where healthy mitochondria give out fluorescence because of J aggregates of JC-1 dyes and damaged cells

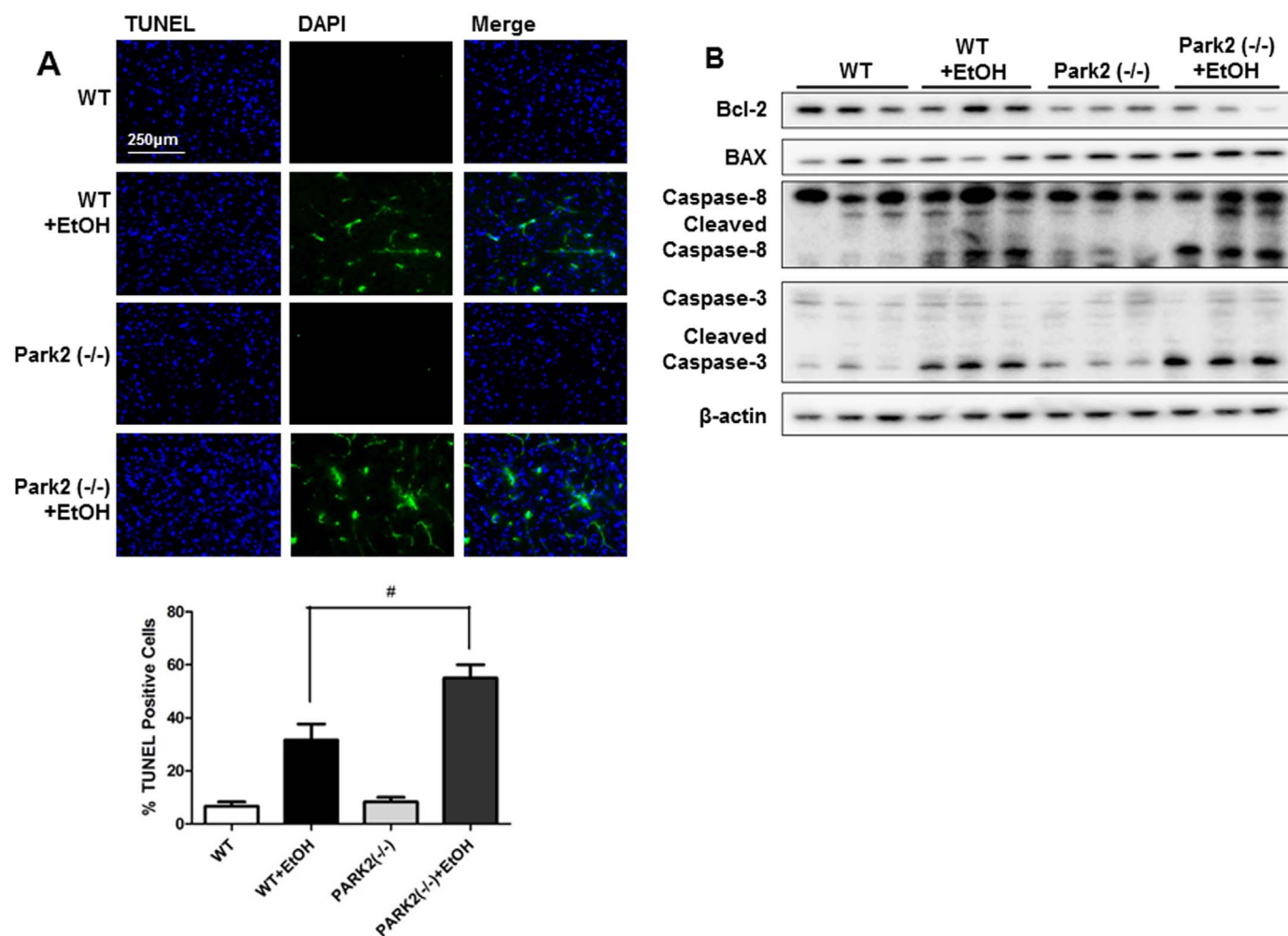


Fig. 5. Park2 deficiency exacerbates ethanol-induced apoptotic cell death. Apoptotic cell death was detected in the brains of four groups as shown by TUNEL staining as described in materials and methods. EtOH-fed Park2 KO mice exhibited a large number of TUNEL-positive cells under the fluorescence microscopy as compared to EtOH-fed Park2 WT mice. The representative stained tissues were viewed with a microscope (X200) (A). Expression of apoptosis related protein (Bcl-2, BAX, Caspase3 and Caspase8) in the brains of four groups was measured. The expressions of proteins were detected by Western blotting using specific antibodies (B). *, < 0.05: Significant difference from control mice and #, $p < 0.05$: Significant difference between the Park2 WT and KO mice.

show green fluorescence because of the lack of mitochondrial membrane potential. Ratio between the measurement at wavelengths of 590 nm (red) and 540 nm (green) fluorescence showing a significantly higher number of damaged cells were observed in the parkin siRNA-transfected PC-12 cells against EtOH treatment (Fig. 6D). Next, we evaluated the amount of the ROS generation in parkin siRNA-transfected PC-12 cells after EtOH treatment (100 μ M). In parkin siRNA-transfected PC-12 cells, EtOH-induced ROS generation was significantly increased by down-regulated Park2 expression (Fig. 6E).

3.7. Effect of p38 MAPK inhibitor on autophagy, mitochondrial function and ROS generation in Park2 KO mice brain and PC-12 cells

We speculated that mitochondria dysfunction and autophagy by Park2 KO might be associated with activation of the p38 MAPK pathway. In support of our assumption, there was a significant increase of p38 MAPK phosphorylation in EtOH-fed Park2 KO mice compared with EtOH-fed Park2 WT mice (Fig. 7A). However, JNK and ERK phosphorylation showed no difference between Park2 KO mice with Park2 WT mice (data not shown). The p38 MAPK protein is essential for the mitochondrial function and formation of ROS in the brains of PD. In order to further examine the mechanisms regulating mitochondrial function by the p38 pathway, EtOH-fed Park2 KO mice were injected with p38 specific inhibitors (10 mg/kg; i.p.), and investigated

for the involvement of the p38 pathway in autophagy protein expression. The p38 inhibitor reversed the Park2 KO mediated reducing effect of autophagy proteins (LC3 and TOM 20) expression in Park2 KO mice brain (Fig. 7B). The ratio of LC3-II/TOM20 in Park2 KO mice brain was also reversed by injection of p38 inhibitor (Fig. 7C). In addition, the effect of p38 inhibitor on mitochondrial membrane potential loss in Park2 KO mice brain was investigated by JC-1 staining. The ratio between the measurement at wavelengths of 590 nm (red) and 540 nm (green) fluorescence showing that EtOH-induced membrane potential loss were significantly decreased by p38 inhibitor treatment (10 μ M) in the Park2 KO mice brain (Fig. 7D). We also evaluated the effect of p38 inhibitor on the amount of EtOH-induced ROS generation in Park2 KO mice brain. EtOH-induced ROS generation was significantly reduced by inhibition of p38 MAPK in Park2 KO mice brain (Fig. 7E and F). The involvement of the p38 pathway was also studied in PC-12 cells. Since the EtOH-induced phosphorylations of p38 were found to be significantly increased in Park2 knock-downed PC-12 cells (Fig. 8A), we employed p38 specific inhibitor to further study the involvement of p38 pathways. The p38 inhibitor reversed the Park2 knock-down mediated promoting effect of autophagy marker proteins (TOM20, LC3 and COX4) expression in PC-12 cells (Fig. 8A). The ratio of LC3-II/TOM20 in parkin siRNA-transfected PC-12 cells was also reversed by treatment of p38 inhibitor (Fig. 8B). In addition, EtOH-induced mitochondrial membrane potential-dependent aggregated JC-1 dye

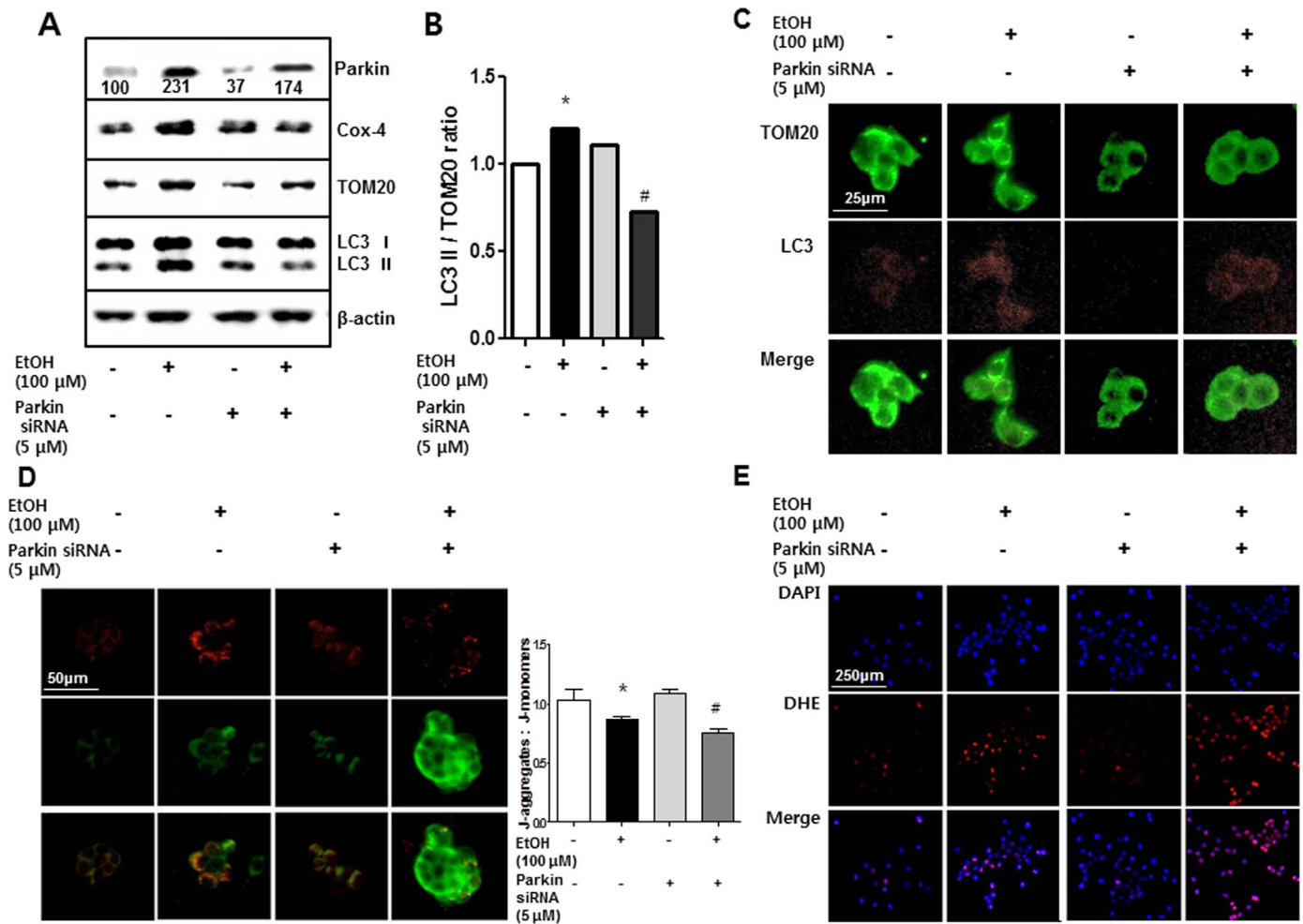


Fig. 6. Knock down of Park2 amplifies EtOH-induced mitochondrial dysfunction and oxidative stress in PC-12 cells. To evaluate relation of Park2 and mitochondrial function and oxidative stress in PC-12 cells, Western blot, double immunofluorescence staining of TOM20 with LC3 was performed. Expression of Parkin (Numbers: percentage of expression), Cox-4, TOM20 and LC3 were examined by specific antibodies in Park2 knock-downed PC-12 cells (A). The ratio of LC3 II/TOM20 was measured for comparison of mitophagy (B). The cells were incubated with specific antibodies against TOM20 (green) and LC3 (red) proteins. The representative stained tissues were viewed with a microscope (X400) (C). Photomicrographs of transmembrane potential-dependent JC-1 staining of mitochondria. High mitochondrial polarization is indicated by red fluorescence due to JC-aggregate formation by the concentrated dye, depolarized regions are indicated by the green fluorescence of JC-1 monomers. The representative stained tissues were viewed with a microscope (X400) (D). Superoxide production was examined by DHE staining in Park2 knock-downed PC-12 cells. The representative stained tissues were viewed with a microscope (X100) (E). *, $p < 0.05$: Significant difference from control mice and #, $p < 0.05$: Significant difference between the Park2 WT and KO mice. (For interpretation of the references to color in this figure legend, the reader is referred to the web version of this article.)

was also significantly decreased by p38 inhibitor treatment in the parkin siRNA-transfected PC-12 cells (Fig. 8C). Next, we evaluated the effect of p38 inhibitor on the amount of EtOH-induced ROS generation in parkin siRNA-transfected PC-12 cells. In parkin siRNA-transfected PC-12 cells, EtOH-induced ROS generation was significantly reduced by inhibition of p38 MAPK (Fig. 8D and E).

4. Discussion

Oxidative stress is considered to be an important condition to promote cell death in response to a variety of signals and pathophysiological situations. Many studies have shown that ROS can induce apoptosis in many different cell systems [44–46]. Therefore, it has been demonstrated that apoptosis in the central nervous system leads to neurodegeneration [47,48]. Heavy EtOH consumption produces profound damage to the brain, heart, liver, pancreas, lungs, bone, skeletal muscles, endocrine, and immune systems [35,49–52]. The developing nervous system is particularly vulnerable to EtOH exposure. A single episode of EtOH intoxication, during the developmental period of synaptogenesis, can trigger widespread apoptotic neurode-

generation in a rat or mouse brain [53,54]. The EtOH-intoxicated infant mouse, therefore, provides an excellent model for studying in vivo apoptotic neurodegeneration [54]. Our present data showed that Park2 deficiency amplified EtOH-induced behavioral disorder, dopamine depletion, superoxide formation, lipid peroxidation, protein oxidation and neuronal cell death. In an in vitro study, EtOH-induced superoxide formation and neuronal apoptosis were significantly increased by knock down of Park2. These data indicate that EtOH-induced superoxide generation could be associated with park2 deficiency-induced neuronal cell death and behavioral function.

In PD conditions, the apoptotic death of dopaminergic neurons can be induced by ROS through disruption of mitochondrial dysfunction. 1-methyl-4-phenylpyridinium (MPP+), a metabolite of 1-methyl-4-phenyl-1,2,3,6-tetrahydropyridine (MPTP), is accumulated within the mitochondria of dopaminergic neurons causing neuronal cell death through increased free radicals contents [55]. In the neuronal cell death, mitochondrial dysfunction by increased mitochondrial potential could result in cell death or autophagy. Impaired mitochondrial function could cause DNA damage [56].

Autophagy is induced by various stress signals, such as exposure to

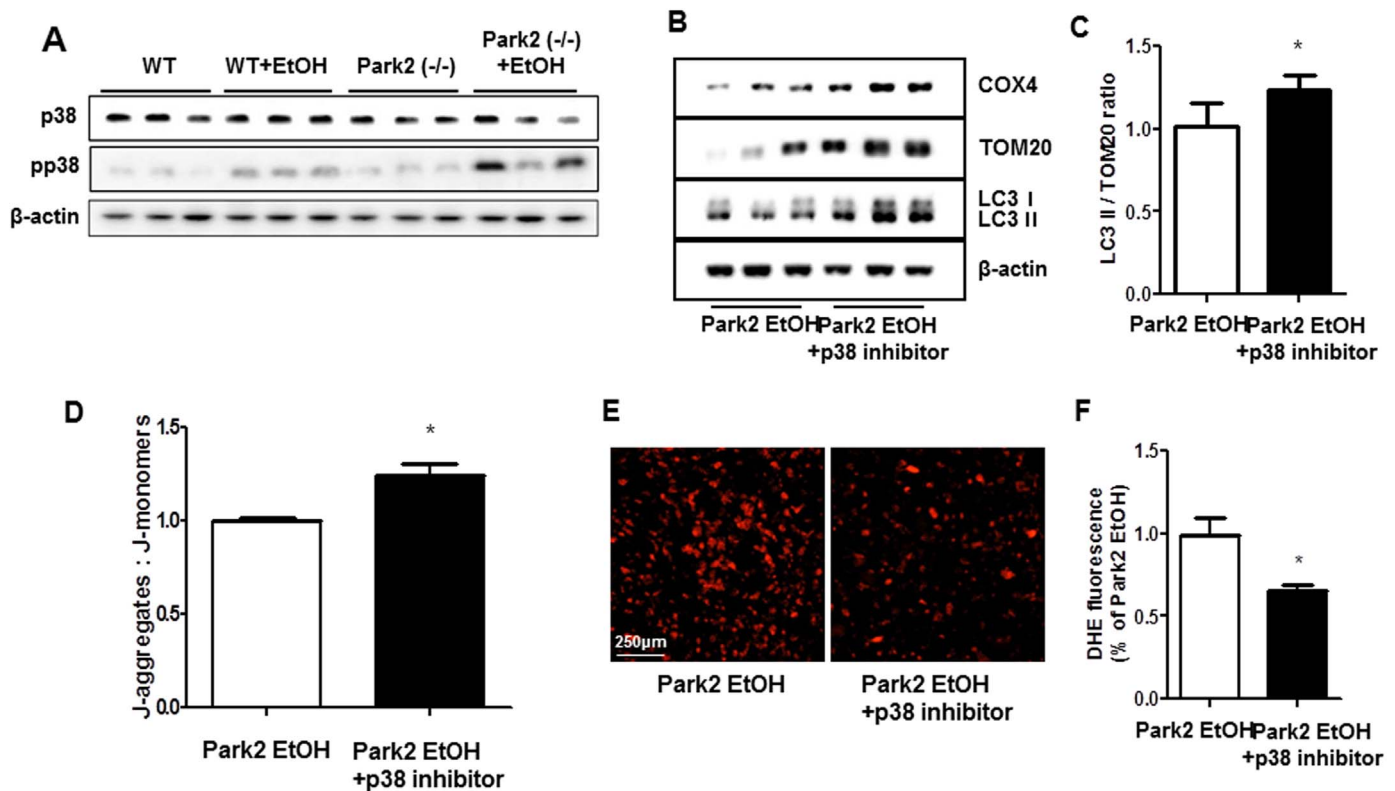


Fig. 7. Effect of p38 MAPK inhibitor SB203580 on park2 deficiency-induced neuro degenerative effects in vivo. The activation of p38 MAPK was measured by Western blot analysis. Expression of p38 MAPK and its phosphorylation form were examined by specific antibodies in the brain (A). Expression of mitochondria function proteins (Cox-4, TOM20 and LC-3) were detected by Western blotting using specific antibodies (B). The ratio of LC3 II/TOM20 was measured for comparison of mitophagy (C). Photomicrographs of transmembrane potential-dependent JC-1 staining of mitochondria. High mitochondrial polarization is indicated by red fluorescence due to JC-aggregate formation by the concentrated dye, depolarized regions are indicated by the green fluorescence of JC-1 monomers (D). Superoxide production was examined by DHE staining between two groups. The representative stained tissues were viewed with a microscope (X100) (E). Accumulation of superoxide were measured by DHE positive fluorescence (F). Each blot is representative for three mice. *, $p < 0.05$: Significant difference between from the injection of p38-specific inhibitors.

toxic agents and metabolic stress [57]. Studies in the past decade have shown that autophagy can also offer protection against numerous pathologies such as neurodegeneration, cardiac disease, diabetes and infections [58,59]. For the survival of healthy neurons, constitutive elimination of damaged proteins by autophagy is an important mechanism [60]. In the aged brain and neurodegenerative diseases such as Alzheimer, Parkinson, and Huntington diseases, disruption of the normal flow autophagy has been shown [60]. In this neuropathies, autophagy is beneficial for clearing toxic factors and enhancing cell survival particularly in neurons [61]. Recently, it was reported that Parkin, a product of park2 gene expression, can eliminate the impaired mitochondria in PD [62]. Parkin is specifically recruited to damaged mitochondria and promotes their autophagic degradation [62]. Other observation shows that these Parkin-marked mitochondrial fragments are LC3 positive, and clearance of damaged mitochondria occurs through Parkin-mediated autophagy. Overexpressed Parkin also eliminates the ROS-induced damaged mitochondria in some PD phenotype animal and cell culture models [63]. In addition, parkin deficiency or mutations lead to oxidative stress and mitochondrial dysfunction. Parkin-null drosophila [13] and mouse [64] strains exhibit mitochondrial impairment and increased oxidative stress. In present study, we demonstrated that park2 KO inhibited autophagy by decrease of mitochondria membrane potential induced by EtOH released ROS in vivo and in vitro. This inhibition is associated with neuronal cell death and behavioral abnormalities. Moreover, these inhibitory effect on autophagy was exacerbated by EtOH exposure. These data indicated that lack of autophagy through inhibition of clearance of damaged mitochondria could be significant in the exacerbation of dopaminergic neurodegeneration in Park2 KO mice.

Recent studies have shown that the EtOH treatment can induce oxidative stress through accumulations of ROS via MAPK signaling [65,66]. Previous studies have shown that EtOH activates MAPK cascades, and increases ROS production related via p38 MAPK pathways [67]. In addition, inhibition of p38 MAPK reduced neuronal death and H_2O_2 production [68]. The activation of p38 MAPK by death receptors has been described by several groups [69]. Moreover, a recent study demonstrated that activation of p38 MAPK can induce mitochondrial potential, caspase activation and cell death [70]. This evidence suggests that p38 MAPK is a very important factor in EtOH-induced cell death and regulation of ROS production. In our present study, Park2 KO mice showed significantly decreased autophagy through highly mitochondrial dysfunction, up-regulated ROS formation and neuronal apoptosis compared to Park2 WT mice and the effects associated with the activation of p38 were increased. However, EtOH-induced mitochondrial dysfunction and ROS formation were significantly reduced by the specific p38 inhibitor in Park2 KO mice. In addition, an in vitro study showed that the exacerbating effect of Park2 knock-down on EtOH-induced mitochondrial dysfunction was significantly reduced by the treatment of p38 specific inhibitor. Therefore, we suggest that park2 deficiency amplifies EtOH-induced neurodegeneration through ROS-dependent up-regulation of p38 activation. A recent study showed that Parkin suppresses tyrosinase-induced apoptotic neuronal cell death through inhibiting p38 activation [71]. These data indicate that down regulation of autophagy could contribute to enhanced neuronal cell damages in Park2 KO mice. This reduced mitochondrial function and autophagy could be involved with ROS formation via p38 MAPK in Park KO mice.

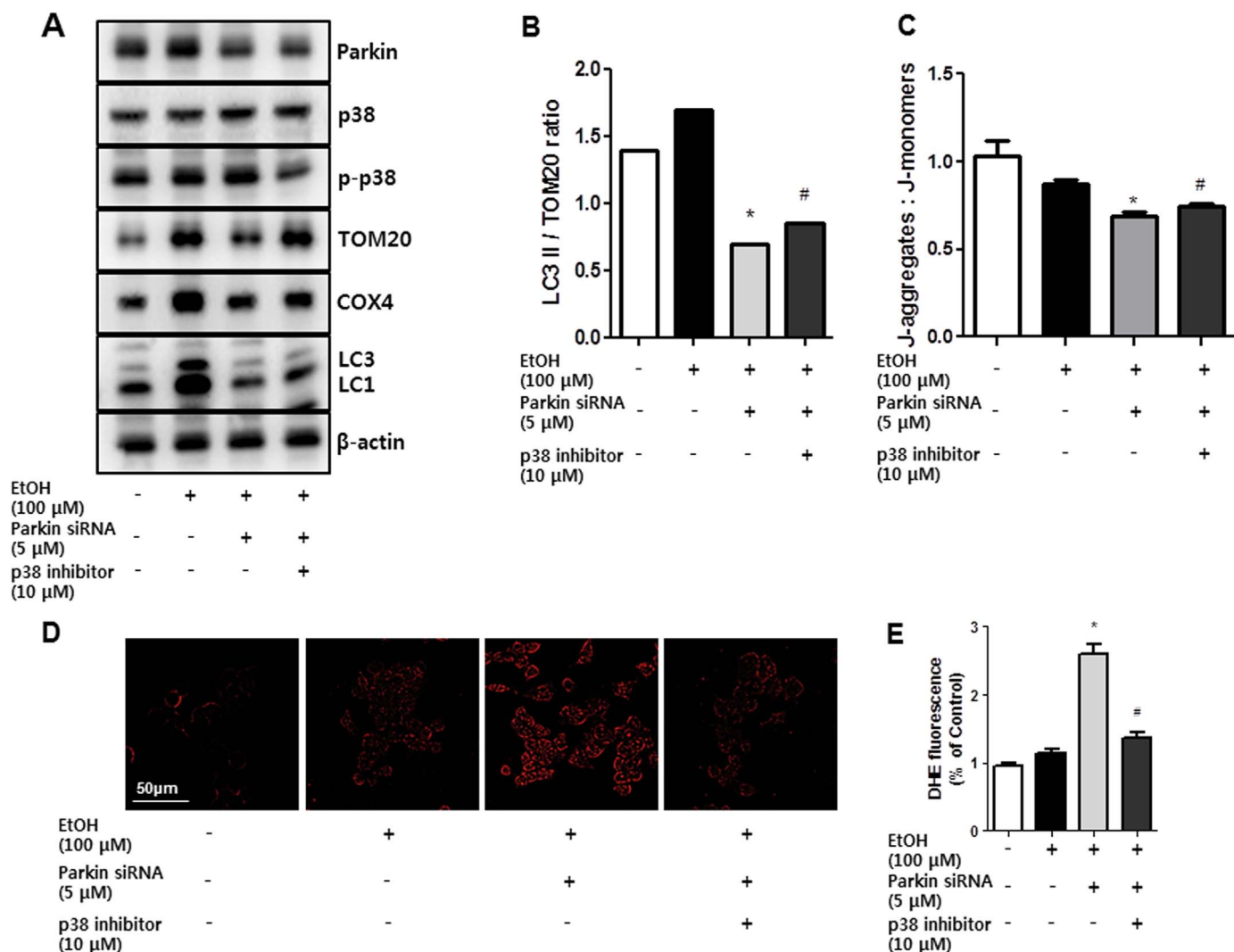


Fig. 8. Involvement of p38 pathway in the exacerbate effect of Park2 deficiency on neurodegeneration. To involvement of p38 pathway in the exacerbate effect of Park2 deficiency, Park2 knock-down PC-12 cells were inhibited with p38 specific inhibitor (10 μM) for 24 h at 37 °C. Expression of parkin, p38 MAPK and its phosphorylation form were examined by specific antibodies (A). Expression of autophagy-related proteins (COX4, TOM20 and LC3) were detected by Western blotting using specific antibodies (A). The ratio of LC3 II/TOM20 was measured for comparison of mitophagy (B). Photomicrographs of transmembrane potential-dependent JC-1 staining of mitochondria. High mitochondrial polarization is indicated by red fluorescence due to JC-aggregate formation by the concentrated dye, depolarized regions are indicated by the green fluorescence of JC-1 monomers (C). Superoxide production was examined by DHE staining in Park2 knock-downed PC-12 cells. The representative stained tissues were viewed with a microscope (X400) (D). Accumulation of superoxide were measured by DHE positive fluorescence (E). *, $p < 0.05$: Significant difference from the Con-siRNA transfected PC-12 cells and #, $p < 0.05$: Significant difference between from the cotreated with p38-specific inhibitors.

5. Conclusion

EtOH consumption can induce the ROS formation through activation of p38 MAPK pathway. This ROS can cause the dopaminergic neurodegeneration through neuronal apoptosis, by inhibition of the autophagy system operating for elimination of damaged cells. However, in Park2 KO mice showed significantly decreased autophagy through highly mitochondrial dysfunction. This study suggests that parkin has a neuroprotective role against oxidative stress mediated damaged mitochondria and autophagy, and parkin deficiency exacerbates ethanol-induced damage in dopaminergic neuron through p38 MAPK pathway.

Conflict of interests

The authors declare no conflict of interest.

Acknowledgements

This work was supported by a grant from the National Research

Foundation of Korea (NRF) funded by the Korean Government (MSIP; MRC, 2008-0062275), by a grant from Marine Biotechnology Program from the Ministry of Oceans and Fisheries, Korea (20150184).

References

- [1] T. Kitada, S. Asakawa, N. Hattori, H. Matsumine, Y. Yamamura, S. Minoshima, M. Yokochi, Y. Mizuno, N. Shimizu, Mutations in the parkin gene cause autosomal recessive juvenile parkinsonism, *Nature* 392 (6676) (1998) 605–608.
- [2] T.M. Dawson, Parkin and defective ubiquitination in Parkinson's disease, *J. Neural Transm. Suppl.* 70 (2006) 209–213.
- [3] D.C. Rubinsztein, The roles of intracellular protein-degradation pathways in neurodegeneration, *Nature* 443 (7113) (2006) 780–786.
- [4] Y. Imai, M. Soda, R. Takahashi, Parkin suppresses unfolded protein stress-induced cell death through its E3 ubiquitin-protein ligase activity, *J. Biol. Chem.* 275 (46) (2000) 35661–35664.
- [5] H. Shimura, N. Hattori, S. Kubo, Y. Mizuno, S. Asakawa, S. Minoshima, N. Shimizu, K. Iwai, T. Chiba, K. Tanaka, T. Suzuki, Familial Parkinson disease gene product, parkin, is a ubiquitin-protein ligase, *Nat. Genet.* 25 (3) (2000) 302–305.
- [6] Y. Zhang, J. Gao, K.K. Chung, H. Huang, V.L. Dawson, T.M. Dawson, Parkin functions as an E2-dependent ubiquitin-protein ligase and promotes the degradation of the synaptic vesicle-associated protein, CDCrel-1, *Proc. Natl. Acad. Sci. USA* 97 (24) (2000) 13354–13359.
- [7] E. Leroy, R. Boyer, G. Auburger, B. Leube, G. Ulm, E. Mezey, G. Harta,

- M.J. Brownstein, S. Jonnalagada, T. Chernova, A. Dehejia, C. Lavedan, T. Gasser, P.J. Steinbach, K.D. Wilkinson, M.H. Polymeropoulos, The ubiquitin pathway in Parkinson's disease, *Nature* 395 (6701) (1998) 451–452.
- [8] D. Sulzer, Multiple hit hypotheses for dopamine neuron loss in Parkinson's disease, *Trends Neurosci.* 30 (5) (2007) 244–250.
- [9] K. Tanaka, T. Suzuki, N. Hattori, Y. Mizuno, Ubiquitin, proteasome and parkin, *Biochim. Biophys. Acta* 1695 (1–3) (2004) 235–247.
- [10] S. Geisler, K.M. Holmstrom, D. Skujat, F.C. Fiesel, O.C. Rothfuss, P.J. Kahle, W. Springer, PINK1/Parkin-mediated mitophagy is dependent on VDAC1 and p62/SQSTM1, *Nat. Cell Biol.* 12 (2) (2010) 119–131.
- [11] I.E. Clark, M.W. Dodson, C. Jiang, J.H. Cao, J.R. Huh, J.H. Seol, S.J. Yoo, B.A. Hay, M. Guo, *Drosophila pink1* is required for mitochondrial function and interacts genetically with parkin, *Nature* 441 (7097) (2006) 1162–1166.
- [12] D. Narendra, A. Tanaka, D.F. Suen, R.J. Youle, Parkin is recruited selectively to impaired mitochondria and promotes their autophagy, *J. Cell Biol.* 183 (5) (2008) 795–803.
- [13] J.C. Greene, A.J. Whitworth, I. Kuo, L.A. Andrews, M.B. Feany, L.J. Pallanck, Mitochondrial pathology and apoptotic muscle degeneration in *Drosophila* parkin mutants, *Proc. Natl. Acad. Sci. USA* 100 (7) (2003) 4078–4083.
- [14] M.S. Goldberg, S.M. Fleming, J.J. Palacino, C. Cepeda, H.A. Lam, A. Bhatnagar, E.G. Meloni, N. Wu, L.C. Ackerson, G.J. Klapstein, M. Gajendiran, B.L. Roth, M.F. Chesselet, N.T. Maidment, M.S. Levine, J. Shen, Parkin-deficient mice exhibit nigrostriatal deficits but not loss of dopaminergic neurons, *J. Biol. Chem.* 278 (44) (2003) 43628–43635.
- [15] C. Henchcliffe, M.F. Beal, Mitochondrial biology and oxidative stress in Parkinson disease pathogenesis, *Nat. Clin. Pract. Neurol.* 4 (11) (2008) 600–609.
- [16] L. Petrucelli, C. O'Farrell, P.J. Lockhart, M. Baptista, K. Kehoe, L. Vink, P. Choi, B. Wolozin, M. Farrer, J. Hardy, M.R. Cookson, Parkin protects against the toxicity associated with mutant alpha-synuclein: proteasome dysfunction selectively affects catecholaminergic neurons, *Neuron* 36 (6) (2002) 1007–1019.
- [17] M. Yamada, Y. Mizuno, H. Mochizuki, Parkin gene therapy for alpha-synucleinopathy: a rat model of Parkinson's disease, *Hum. gene Ther.* 16 (2) (2005) 262–270.
- [18] Y. Yang, I. Nishimura, Y. Imai, R. Takahashi, B. Lu, Parkin suppresses dopaminergic neuron-selective neurotoxicity induced by Pael-R in *Drosophila*, *Neuron* 37 (6) (2003) 911–924.
- [19] L. Verccammen, A. Van der Perren, E. Vaudano, R. Gijssbers, Z. Debyser, C. Van den Haute, V. Baekelandt, Parkin protects against neurotoxicity in the 6-hydroxydopamine rat model for Parkinson's disease, *Mol. Ther.: J. Am. Soc. Gene Ther.* 14 (5) (2006) 716–723.
- [20] H. Jiang, Y. Ren, J. Zhao, J. Feng, Parkin protects human dopaminergic neuroblastoma cells against dopamine-induced apoptosis, *Hum. Mol. Genet.* 13 (16) (2004) 1745–1754.
- [21] M. Hayyan, M.A. Hashim, I.M. AlNashef, Superoxide ion: generation and chemical implications, *Chem. Rev.* 116 (5) (2016) 3029–3085.
- [22] T.P. Devasagayam, J.C. Tilak, K.K. Boloor, K.S. Sane, S.S. Ghaskadbi, R.D. Lele, Free radicals and antioxidants in human health: current status and future prospects, *J. Assoc. Physicians India* 52 (2004) 794–804.
- [23] A. Kulisz, N. Chen, N.S. Chandel, Z. Shao, P.T. Schumacker, Mitochondrial, ROS initiate phosphorylation of p38 MAP kinase during hypoxia in cardiomyocytes, *Am. J. Physiol. Lung Cell. Mol. Physiol.* 282 (6) (2002) L1324–L1329.
- [24] W. Zhang, T. Wang, Z. Pei, D.S. Miller, X. Wu, M.L. Block, B. Wilson, W. Zhang, Y. Zhou, J.S. Hong, J. Zhang, Aggregated alpha-synuclein activates microglia: a process leading to disease progression in Parkinson's disease, *FASEB J.: Off. Publ. Fed. Am. Soc. Exp. Biol.* 19 (6) (2005) 533–542.
- [25] J.A. McCubrey, M.M. Lahair, R.A. Franklin, Reactive oxygen species-induced activation of the MAP kinase signaling pathways, *Antioxid. Redox Signal.* 8 (9–10) (2006) 1775–1789.
- [26] M. Torres, H.J. Forman, Redox signaling and the MAP kinase pathways, *BioFactors* 17 (1–4) (2003) 287–296.
- [27] R.M. Silva, C.Y. Kuan, P. Rakic, R.E. Burke, Mixed lineage kinase-c-jun N-terminal kinase signaling pathway: a new therapeutic target in Parkinson's disease, *Mov. Disord.: Off. J. Mov. Disord. Soc.* 20 (6) (2005) 653–664.
- [28] J.E. Chipuk, D.R. Green, How do BCL-2 proteins induce mitochondrial outer membrane permeabilization?, *Trends Cell Biol.* 18 (4) (2008) 157–164.
- [29] S. Karunakaran, U. Saeed, M. Mishra, R.K. Valli, S.D. Joshi, D.P. Meka, P. Seth, V. Ravindranath, Selective activation of p38 mitogen-activated protein kinase in dopaminergic neurons of substantia nigra leads to nuclear translocation of p53 in 1-methyl-4-phenyl-1,2,3,6-tetrahydropyridine-treated mice, *J. Neurosci.: Off. J. Soc. Neurosci.* 28 (47) (2008) 12500–12509.
- [30] N. Farley, G. Pedraza-Alva, D. Serrano-Gomez, V. Nagaleekar, A. Aronshtam, T. Krahl, T. Thornton, M. Rincon, p38 mitogen-activated protein kinase mediates the Fas-induced mitochondrial death pathway in CD8+ T cells, *Mol. Cell. Biol.* 26 (6) (2006) 2118–2129.
- [31] Q. Jiang, F. Li, K. Shi, P. Wu, J. An, Y. Yang, C. Xu, Involvement of p38 in signal switching from autophagy to apoptosis via the PERK/eIF2alpha/ATF4 axis in selenite-treated NB4 cells, *Cell Death Dis.* 5 (2014) e1270.
- [32] E. Keil, R. Hocker, M. Schuster, F. Essmann, N. Ueffing, B. Hoffman, D.A. Liebermann, K. Pfeffer, K. Schulze-Osthoff, I. Schmitz, Phosphorylation of Atg5 by the Gadd45beta-MEKK4-p38 pathway inhibits autophagy, *Cell Death Differ.* 20 (2) (2013) 321–332.
- [33] V. Calabrese, G. Scapagnini, S. Latteri, C. Colombrita, A. Ravagna, C. Catalano, G. Pennisi, M. Calvani, D.A. Butterfield, Long-term ethanol administration enhances age-dependent modulation of redox state in different brain regions in the rat: protection by acetyl carnitine, *Int. J. Tissue React.* 24 (3) (2002) 97–104.
- [34] I. Diamond, A.S. Gordon, Cellular and molecular neuroscience of alcoholism, *Physiol. Rev.* 77 (1) (1997) 1–20.
- [35] J.B. Hoek, A. Cahill, J.G. Pastorino, Alcohol and mitochondria: a dysfunctional relationship, *Gastroenterology* 122 (7) (2002) 2049–2063.
- [36] S.D. Skaper, M. Floreani, M. Cecon, L. Facci, P. Giusti, Excitotoxicity, oxidative stress, and the neuroprotective potential of melatonin, *Ann. N.Y. Acad. Sci.* 890 (1999) 107–118.
- [37] D.Y. Choi, M.K. Lee, J.T. Hong, Lack of CCR5 modifies glial phenotypes and population of the nigral dopaminergic neurons, but not MPTP-induced dopaminergic neurodegeneration, *Neurobiol. Dis.* 49C (2012) 159–168.
- [38] D.Y. Choi, M. Liu, R.L. Hunter, W.A. Cass, J.D. Pandya, P.G. Sullivan, E.J. Shin, H.C. Kim, D.M. Gash, G. Bing, Striatal neuroinflammation promotes Parkinsonism in rats, *PLoS One* 4 (5) (2009) e5482.
- [39] H. Xu, G.K. Gouras, J.P. Greenfield, B. Vincent, J. Naslund, L. Mazzarelli, G. Fried, J.N. Jovanovic, M. Seeger, N.R. Relkin, F. Liao, F. Checler, J.D. Buxbaum, B.T. Chait, G. Thinakaran, S.S. Sisodia, R. Wang, P. Greengard, S. Gandy, Estrogen reduces neuronal generation of Alzheimer beta-amyloid peptides, *Nat. Med.* 4 (4) (1998) 447–451.
- [40] G.C. Kujoth, A. Hiona, T.D. Pugh, S. Someya, K. Panzer, S.E. Wohlgemuth, T. Hofer, A.Y. Seo, R. Sullivan, W.A. Jobling, J.D. Morrow, H. Van Remmen, J.M. Sedivy, T. Yamasoba, M. Tanokura, R. Weindruch, C. Leeuwenburgh, T.A. Prolla, Mitochondrial, DNA mutations, oxidative stress, and apoptosis in mammalian aging, *Science* 309 (5733) (2005) 481–484.
- [41] G. Tsai, D.C. Goff, R.W. Chang, J. Flood, L. Baer, J.T. Coyle, Markers of glutamatergic neurotransmission and oxidative stress associated with tardive dyskinesia, *Am. J. Psychiatry* 155 (9) (1998) 1207–1213.
- [42] I. Tanida, T. Ueno, E. Kominami, LC3 and autophagy, *Methods Mol. Biol.* 445 (2008) 77–88.
- [43] N. Mizushima, T. Yoshimori, How to interpret LC3 immunoblotting, *Autophagy* 3 (6) (2007) 542–545.
- [44] L. Wang, T. Hu, J. Shen, L. Zhang, L.F. Li, R.L. Chan, M.X. Li, W.K. Wu, C.H. Cho, Mitronone induced mitochondrial dysfunction and ROS-dependent apoptosis in colon cancer cells, *Life Sci.* (2016).
- [45] M. Koul, S. Meena, A. Kumar, P.R. Sharma, V. Singamaneni, S. Riyaz-Ul-Hassan, A. Hamid, A. Chaubey, A. Prabhakar, P. Gupta, S. Singh, Secondary metabolites from endophytic fungus penicillium pinophilum induce ROS-mediated apoptosis through mitochondrial pathway in pancreatic cancer cells, *Planta Med.* 82 (4) (2016) 344–355.
- [46] H. Cui, S. Wu, Y. Shang, Z. Li, M. Chen, F. Li, C. Wang, Pleurotus nebrodensis polysaccharide (PN50G) evokes A549 cell apoptosis by the ROS/AMPK/P13K/AKT/mTOR pathway to suppress tumor growth, *Food Funct.* 7 (3) (2016) 1616–1627.
- [47] R.J. Braun, Mitochondrion-mediated cell death: dissecting yeast apoptosis for a better understanding of neurodegeneration, *Front. Oncol.* 2 (2012) 182.
- [48] I.C. Stefani, D. Wright, K.M. Polizzi, C. Kontoravdi, The role of ER stress-induced apoptosis in neurodegeneration, *Curr. Alzheimer Res.* 9 (3) (2012) 373–387.
- [49] P.A. May, J. Blankenship, A.S. Marais, J.P. Gossage, W.O. Kalberg, B. Joubert, M. Cloete, R. Barnard, M. De Vries, J. Hasken, L.K. Robinson, C.M. Adams, D. Buckley, M. Manning, C.D. Parry, H.E. Hoyme, B. Tabachnick, S. Seedat, Maternal alcohol consumption producing fetal alcohol spectrum disorders (FASD): quantity, frequency, and timing of drinking, *Drug Alcohol Depend.* 133 (2) (2013) 502–512.
- [50] E.P. Riley, M.A. Infante, K.R. Warren, Fetal alcohol spectrum disorders: an overview, *Neuropsychol. Rev.* 21 (2) (2011) 73–80.
- [51] P.D. Sampson, A.P. Streissguth, F.L. Bookstein, H.M. Barr, On categorizations in analyses of alcohol teratogenesis, *Environ. Health Perspect.* 108 (Suppl 3) (2000) 421–428.
- [52] P.D. Sampson, A.P. Streissguth, F.L. Bookstein, R.E. Little, S.K. Clarren, P. Dehaene, J.W. Hanson, J.M. Graham Jr., Incidence of fetal alcohol syndrome and prevalence of alcohol-related neurodevelopmental disorder, *Teratology* 56 (5) (1997) 317–326.
- [53] J.W. Olney, T. Tenkova, K. Dikranian, L.J. Muglia, W.J. Jermakowicz, C. D'Sa, K.A. Roth, Ethanol-induced caspase-3 activation in the in vivo developing mouse brain, *Neurobiol. Dis.* 9 (2) (2002) 205–219.
- [54] C. Ikonomidou, P. Bittigau, M.J. Ishimaru, D.F. Wozniak, C. Koch, K. Genz, M.T. Price, V. Stefovskaja, F. Horster, T. Tenkova, K. Dikranian, J.W. Olney, Ethanol-induced apoptotic neurodegeneration and fetal alcohol syndrome, *Science* 287 (5455) (2000) 1056–1060.
- [55] J.A. Dykens, Isolated cerebral and cerebellar mitochondria produce free radicals when exposed to elevated CA2+ and Na+: implications for neurodegeneration, *J. Neurochem.* 63 (2) (1994) 584–591.
- [56] S.M. de la Monte, T. Luong, T.R. Neely, D. Robinson, J.R. Wands, Mitochondrial, DNA damage as a mechanism of cell loss in Alzheimer's disease, *Lab. Invest.; a J. Tech. Methods Pathol.* 80 (8) (2000) 1323–1335.
- [57] H.M. Shen, P. Codogno, Autophagy is a survival force via suppression of necrotic cell death, *Exp. Cell Res.* 318 (11) (2012) 1304–1308.
- [58] S. Sridhar, Y. Botbol, F. Macian, A.M. Cuervo, Autophagy and disease: always two sides to a problem, *J. Pathol.* 226 (2) (2012) 255–273.
- [59] Y. Feng, D. He, Z. Yao, D.J. Klionsky, The machinery of macroautophagy, *Cell Res.* 24 (1) (2014) 24–41.
- [60] M. Xilouri, L. Stefanis, Autophagy in the central nervous system: implications for neurodegenerative disorders, *CNS Neurol. Disord. Drug Targets* 9 (6) (2010) 701–719.
- [61] J.A. Lee, Neuronal autophagy: a housekeeper or a fighter in neuronal cell survival?, *Exp. Neurobiol.* 21 (1) (2012) 1–8.
- [62] A. Tanaka, Parkin-mediated selective mitochondrial autophagy, mitophagy: Parkin purges damaged organelles from the vital mitochondrial network, *FEBS Lett.* 584 (7) (2010) 1386–1392.
- [63] T. Gasser, Mendelian forms of Parkinson's disease, *Biochim. Biophys. Acta* 1792 (7)

- (2009) 587–596.
- [64] J.J. Palacino, D. Sagi, M.S. Goldberg, S. Krauss, C. Motz, M. Wacker, J. Klose, J. Shen, Mitochondrial dysfunction and oxidative damage in parkin-deficient mice, *J. Biol. Chem.* 279 (18) (2004) 18614–18622.
- [65] Y. Morio, M. Tsuji, M. Inagaki, M. Nakagawa, Y. Asaka, H. Oyamada, K. Furuya, K. Oguchi, Ethanol-induced apoptosis in human liver adenocarcinoma cells (SK-Hep1): fas- and mitochondria-mediated pathways and interaction with MAPK signaling system, *Toxicol. Vitro: Int. J. Publ. Assoc. BIBRA* 27 (6) (2013) 1820–1829.
- [66] W. Gao, P. Zhou, X. Ma, B. Tschudy-Seney, J. Chen, N.L. Magner, A. Revzin, J.A. Nolte, M.A. Zern, Y. Duan, Ethanol negatively regulates hepatic differentiation of hESC by inhibition of the MAPK/ERK signaling pathway in vitro, *PLoS One* 9 (11) (2014) e112698.
- [67] T. Yan, Y. Zhao, X. Zhang, Acetaldehyde induces cytotoxicity of SH-SY5Y cells via inhibition of Akt activation and induction of Oxidative stress, *Oxid. Med. Cell. Longev.* 2016 (2016) 4512309.
- [68] D. Davila, I. Torres-Aleman, Neuronal death by oxidative stress involves activation of FOXO3 through a two-arm pathway that activates stress kinases and attenuates insulin-like growth factor I signaling, *Mol. Biol. Cell* 19 (5) (2008) 2014–2025.
- [69] K. Ono, J. Han, The p38 signal transduction pathway: activation and function, *Cell. Signal.* 12 (1) (2000) 1–13.
- [70] B. Brenner, U. Koppenhoefer, C. Weinstock, O. Linderkamp, F. Lang, E. Gulbins, Fas- or ceramide-induced apoptosis is mediated by a Rac1-regulated activation of Jun N-terminal kinase/p38 kinases and GADD153, *J. Biol. Chem.* 272 (35) (1997) 22173–22181.
- [71] T. Hasegawa, A. Treis, N. Patenge, F.C. Fiesel, W. Springer, P.J. Kahle, Parkin protects against tyrosinase-mediated dopamine neurotoxicity by suppressing stress-activated protein kinase pathways, *J. Neurochem.* 105 (5) (2008) 1700–1715.